

Molecular Characterization of an NADPH-Dependent Acetoin Reductase/2,3-Butanediol Dehydrogenase from *Clostridium beijerinckii* NCIMB 8052

John Raedts, Marco A. J. Siemerink,* Mark Levisson, John van der Oost, Servé W. M. Kengen

Laboratory of Microbiology, Wageningen University and Research Centre, Wageningen, The Netherlands

Acetoin reductase is an important enzyme for the fermentative production of 2,3-butanediol, a chemical compound with a very broad industrial use. Here, we report on the discovery and characterization of an acetoin reductase from *Clostridium beijerinckii* NCIMB 8052. An *in silico* screen of the *C. beijerinckii* genome revealed eight potential acetoin reductases. One of them (CBEI_1464) showed substantial acetoin reductase activity after expression in *Escherichia coli*. The purified enzyme (*C. beijerinckii* acetoin reductase [Cb-ACR]) was found to exist predominantly as a homodimer. In addition to acetoin (or 2,3-butanediol), other secondary alcohols and corresponding ketones were converted as well, provided that another electronegative group was attached to the adjacent C-3 carbon. Optimal activity was at pH 6.5 (reduction) and 9.5 (oxidation) and around 68°C. Cb-ACR accepts both NADH and NADPH as electron donors; however, unlike closely related enzymes, NADPH is preferred (K_m , 32 μ M). Cb-ACR was compared to characterized close homologs, all belonging to the “threonine dehydrogenase and related Zn-dependent dehydrogenases” (COG1063). Metal analysis confirmed the presence of 2 Zn²⁺ atoms. To gain insight into the substrate and cofactor specificity, a structural model was constructed. The catalytic zinc atom is likely coordinated by Cys₃₇, His₇₀, and Glu₇₁, while the structural zinc site is probably composed of Cys₁₀₀, Cys₁₀₃, Cys₁₀₆, and Cys₁₁₄. Residues determining NADP specificity were predicted as well. The physiological role of Cb-ACR in *C. beijerinckii* is discussed.

Clostridia are well known for their capacity to produce various acids and alcohols as end products of the anaerobic breakdown of different polysaccharides (1). These fermentation products are of interest as building blocks in the chemical industry or as biofuels. A renowned example, which has been studied extensively in the past, is the production of acetone, 1-butanol, and ethanol (ABE) by solventogenic clostridia. This process, also known as ABE fermentation, has been studied extensively in the past (2). In addition to ABE, some clostridial species, like *Clostridium beijerinckii* or *Clostridium acetobutylicum*, are able to produce isopropanol or acetoin, respectively (3). Acetoin can be converted to 2,3-butanediol via a single reduction step, catalyzed by acetoin reductase (ACR) (or 2,3-butanediol dehydrogenase [BDH]; EC 1.1.1.4). Acetoin and 2,3-butanediol are well-known metabolic end products of various microorganisms, and their biosynthesis in most cases involves pyruvate and α -acetolactate as intermediates (4, 5). Alternatively, both molecules may also be degraded by certain microorganisms (6). Although many microorganisms, including eukaryotes, are known to interconvert acetoin and 2,3-butanediol, only a few enzymes have actually been characterized in detail (7, 8). 2,3-Butanediol and especially the pure enantiomeric forms are very valuable for the synthesis of chiral high-value pharmaceuticals. Alternatively, 2,3-butanediol may be enzymatically converted into 2-butanol, a potential biofuel with the same energetic value as 1-butanol but with less toxicity to the fermenting organism (1).

Although wild-type *C. acetobutylicum* is known to produce acetoin (3), it is not able to produce 2,3-butanediol (9). However, heterologous expression of an acetoin reductase from *C. beijerinckii* enabled production of 2,3-butanediol, as has recently been shown by Siemerink et al. (10). Acetoin reductases are alcohol dehydrogenases (ADHs; EC 1.1.1), a large group of enzymes which are found in all three domains of life and which are capable

of catalyzing the reversible reaction between aldehydes and ketones and their corresponding alcohols (11, 12). Clostridia harbor many putative ADH gene sequences, but the specificity of the corresponding enzymes can often not be concluded from the primary structure. Most characterized ACRs/BDHs belong to the superfamily of medium-chain dehydrogenases/reductases (MDRs), although some belong to the short-chain dehydrogenases (SDHs) (13).

This work reports on the discovery and detailed characterization of the acetoin reductase from *C. beijerinckii* NCIMB 8052, which was previously used to enable 2,3-butanediol production in *C. acetobutylicum* (10). The enzyme was selected from a set of eight putative acetoin reductases, six of which were heterologously expressed in *Escherichia coli* and analyzed for the desired activity. The selected enzyme was purified to homogeneity and characterized with respect to substrate specificity, temperature and pH optima, kinetics, and structural modeling. Its characteristics are compared to those of related characterized enzymes of the MDR superfamily.

Received 3 December 2013 Accepted 12 January 2014

Published ahead of print 17 January 2014

Editor: R. E. Parales

Address correspondence to Servé W. M. Kengen, serve.kengen@wur.nl.

* Present address: Marco A. J. Siemerink, MicCell Bioservices, Doetinchem, The Netherlands.

J.R. and M.A.J.S. contributed equally to this work.

Supplemental material for this article may be found at <http://dx.doi.org/10.1128/AEM.04007-13>.

Copyright © 2014, American Society for Microbiology. All Rights Reserved.

doi:10.1128/AEM.04007-13

MATERIALS AND METHODS

Materials used. All chemicals were analytical grade and purchased from Sigma-Aldrich (unless stated otherwise). Primers were obtained from Biolegio (Nijmegen, The Netherlands). The restriction enzymes were obtained from Invitrogen (Breda, The Netherlands). For heterologous expression, the vectors pET24d and pET26d (kanamycin resistance; Merck Millipore, Darmstadt, Germany) were used.

Organisms and growth conditions. *E. coli* DH5 α (New England Biolabs, Ipswich, MA, USA) was used as a host for the cloning vectors, and *E. coli* BL21(DE3) was used as an overproduction strain to obtain recombinant protein for purification. All *E. coli* strains were grown at 37°C, 200 rpm, in Luria-Bertani (LB) medium supplemented with MgSO₄ (1 mM), kanamycin (50 μ g/ml), and ZnSO₄ (250 μ M) (unless stated otherwise). Additional zinc was added to ensure full occupancy of the zinc binding sites of the enzyme (14), and additional magnesium was added to increase *E. coli* biomass (15).

Identification and cloning of potential acetoin reductase-encoding genes. The genome of *C. beijerinckii* NCIMB 8052 was screened for potential acetoin reductases by performing BLAST-P searches with the sequences from a set of characterized acetoin reductase/2,3-butanediol dehydrogenases from different organisms (*Bacillus subtilis* subsp. *subtilis* GI:16077691, *Saccharomyces cerevisiae* GI:330443361, *Thermoanaerobacter brockii* GI:1771790, and *Klebsiella pneumoniae* GI:1468939), including the closely related Gram-positive *Bacillus cereus* YUF-4 (GI:14475601) (<http://www.ncbi.nlm.nih.gov/blast>) (16, 17). The putative acetoin reductase genes, *CBEI_0223*, *CBEI_0685*, *CBEI_1464* (*C. beijerinckii* ACR [Cb-ACR]), *CBEI_2243*, *CBEI_3864*, and *CBEI_3890*, were amplified by PCR on *C. beijerinckii* genomic DNA using the indicated primers (see Table S1 in the supplemental material). All PCR products were ligated into their corresponding pET24d or pET26b vector. The cloned genes did not contain a stop codon, resulting in a hexahistidine tag at the C terminus of the enzymes after expression. Chemically competent *E. coli* DH5 α cells were transformed with the ligation mixtures according to the manufacturer's protocol and selected for kanamycin resistance. Colonies were checked by colony PCR, after which restriction analysis and sequence analysis confirmed the correct constructs. Chemically competent *E. coli* BL21(DE3) cells were transformed with the resulting pWUR plasmids (see Table S2 in the supplemental material).

Production and purification of heterologously expressed Cb-ACR. For screening the candidate acetoin reductases, *E. coli* BL21(DE3), containing the different pWUR plasmids, was used to inoculate a 5-ml overnight LB medium culture with the mentioned supplements. This preculture was used to inoculate 50 ml LB medium in conical flasks and incubated for 8 h (37°C, 120 rpm). After 8 h of growth, the cultures were placed on ice for 1 h to induce host chaperones (18) and subsequently induced by adding 0.5 mM isopropyl- β -D-1-thiogalactopyranoside (IPTG). *E. coli* cells were harvested after 15 h of growth at 20°C and resuspended in 20 mM Tris-HCl buffer, pH 7.5, containing 1 mM tris(2-carboxyethyl)phosphine (TCEP) as a reducing agent (19). After three cycles of sonication (20 W for 20 s; intermittent cooling on ice for 30 s), the total cell extract was centrifuged (30 min; 16,000 \times g; 4°C), resulting in a clear cell extract. The crude cell extracts were used for screening purposes.

To overproduce Cb-ACR, a 2-liter culture of *E. coli* BL21(DE3) harboring pWUR450 was grown and induced as described above. The collected cell suspension was treated twice with a French pressure cell (110 MPa), centrifuged for 20 min (16,500 \times g; 4°C), and passed through a 0.45- μ m filter (Sartorius Stedim Biotech). The resulting cell extract was applied to a 20-ml Matrex Gel Red A affinity column (Amicon) equilibrated with 20 mM Tris-HCl buffer (pH 7.5) (buffer A). Unbound protein was removed by washing with 2 column volumes of buffer A, and the recombinant protein was eluted using a linear gradient of 0 to 2 M NaCl in the same buffer. The fractions containing Cb-ACR activity were pooled and applied to a Ni-chelating column (20 ml) equilibrated in buffer A, containing 300 mM NaCl with a flow rate of 2 ml min⁻¹. Proteins were eluted with a linear gradient of 20 to 500 mM imidazole, and fractions (10

ml) were collected. The fractions with highest acetoin reductase activity were pooled and applied at a flow rate of 10 ml min⁻¹ to a HiPrep desalting column (53 ml) (GE Healthcare Europe GmbH, Belgium), equilibrated in buffer A. The desalted fractions were supplemented with 1 mM TCEP and frozen at -20°C under anaerobic conditions.

Screening for acetoin reductase activity. An initial screening for D/L-acetoin reduction was performed with crude cell extracts. Each reduction reaction was performed in a degassed reaction mixture containing 100 mM NaP_i buffer (pH 6.5), 50 mM D/L-acetoin, and 0.28 mM NAD(P)H as described below. The following were included as controls: (i) crude cell extract of *E. coli* BL21(DE3) harboring an empty pET24d vector and (ii) a blank with no substrate. A correction was made for the temperature-dependent spontaneous degradation of NAD(P)H. The reactions in this screening were initiated by adding D/L-acetoin.

Acetoin reductase activity assays. Alcohol oxidations and aldehyde/ketone reductions were determined by following either the reduction of NAD(P)⁺ or the oxidation of NAD(P)H at 340 nm, using a Hitachi U2010 spectrophotometer equipped with a temperature-controlled cuvette holder. Unless stated otherwise, all reactions were performed at 37°C under standard reaction conditions as described below. Each oxidation reaction was performed in a degassed reaction mixture containing 100 mM glycine-NaOH buffer (pH 9.5), 50 mM alcohol, and 0.28 mM NAD(P)⁺. Each reduction reaction was performed in a degassed reaction mixture containing 100 mM sodium phosphate buffer (pH 6.5), 50 mM aldehyde or ketone, and 0.28 mM NAD(P)H.

In all assays, the reaction was initiated by the addition of an appropriate amount of purified enzyme. One unit of Cb-ACR was defined as the amount of enzyme that oxidized or reduced 1 micromole of NAD(P)H or NAD(P)⁺ per minute, respectively. A correction was made for the (temperature-dependent) spontaneous degradation of NAD(P)H. The protein concentration was determined using the Bradford reagent (Bio-Rad) with bovine serum albumin as a standard (20).

Optimal pH and temperature. The optimal pH of the reduction reaction was determined using a 100 mM NaP_i buffer (pH 5.5 to 7.5). The oxidation reaction was determined using a 100 mM glycine-NaOH buffer (pH 8.0 to 10.0). Both reactions were done at 37°C. The optimal temperature of the oxidation and reduction reaction was determined (range, 20°C to 85°C) using the 100 mM NaP_i buffer (pH 6.5) or the 100 mM glycine-NaOH buffer (pH 9.5), respectively. The pH of the buffers was set at 25°C, and temperature corrections were made using their temperature coefficients (± 0.0028 pH/°C for sodium phosphate buffer and ± 0.025 pH/°C for the glycine buffer).

Substrate specificity and kinetics. The activity of purified Cb-ACR was tested on various potential substrates, in either the reductive or the oxidative direction, as described above for the general assay. Kinetic parameters were determined using acetoin as the substrate. Multiple measurements with D/L-acetoin were done (0.0244 mM, 0.0488 mM, 0.098 mM, 0.19 mM, 0.391 mM, 0.781 mM, 1.563 mM, 3.125 mM, 12.5 mM, and 50.0 mM) in the presence of 0.28 mM NAD(P)H. In addition, multiple measurements were performed with the cofactors NADH and NADPH (0.014 mM, 0.028 mM, 0.035 mM, 0.042 mM, 0.056 mM, 0.070 mM, 0.14 mM, and 0.28 mM). The K_m and V_{max} values were calculated by a computer-aided direct fit to the Michaelis-Menten equation. Variability is expressed as standard error of the mean. All reactions followed Michaelis-Menten-type kinetics.

Size exclusion chromatography. The molecular mass of the native enzyme was determined by size exclusion chromatography on a Superdex 200 high-resolution 10/30 column (24 ml; GE Healthcare Europe GmbH, Belgium) equilibrated in 50 mM Tris-HCl containing 100 mM NaCl (pH 7.8). In total, 250 μ l purified enzyme in 50 mM Tris-HCl buffer (pH 7.8) was applied to the column. Proteins used for calibration were Blue dextran 2000 (>2,000 kDa), aldolase (158 kDa), bovine serum albumin (67 kDa), ovalbumin (43 kDa), chymotrypsinogen (25 kDa), and RNase A (13.7 kDa).

TABLE 1 Overview of characterized acetoin reductases/2,3-butanediol dehydrogenases and threonine dehydrogenases

Organism	GI (gene identifier)	COG	Molecular mass, kDa (no. of residues)	Quaternary structure	Activity for ACR/BDH ^a	Activity for TDH ^b	Coenzyme	PDB accession no.	Reference(s)
<i>C. beijerinckii</i> (Cb-ACR)	149902809	1063	38.84 (360)	α2	100/0/99	0	NADP		This paper
<i>B. cereus</i> YUF-4	14475601	1063	38.10 (349)	α2	+ / + / -	ND ^d	NAD		17
<i>P. polymyxa</i>	317183731	1063	37.84 (350)	α2	100/0/72	ND	NAD		37
<i>B. subtilis</i> subsp. <i>subtilis</i> 168	16077691	1063	37.34 (346)	ND	100/1/ND	ND	NAD		52, 53
<i>Mycobacterium</i> strain B-009	327442548	1063	36.78 (350)	α2	100/4/61	ND	NAD		54
<i>S. cerevisiae</i>	330443361	1063	41.45 (382)	α2	100/0/43		NAD		55
<i>T. kodakarensis</i>	57640851	1063	38.10 (350)	α4	ND	+	NAD	3GFB	39, 56
<i>P. furiosus</i>	18893044	1063	37.82 (348)	α4	+	+	NAD		42
<i>E. coli</i>	135560	1063	37.24 (341)	α4	ND	+	NAD		57
<i>T. guaymasensis</i>	317411316	1063	39.53 (365)	α4	98/17/100	-	NADP		36
<i>T. brockii</i>	1771790	1063	37.78 (353)	α4	100/1/ND	ND	NADP	1YKF/1BXZ	41, 53, 58
<i>C. beijerinckii</i> (CbADH) ^c	60592974	1063	37.72 (351)	α4	100/1/0	ND	NADP	1KEV	41, 53, 58
<i>K. pneumoniae</i>	1468939	1028	26.64 (256)	α4	0/0/98	ND	NAD	1GEG	13

^a Specificity of the 2,3-butanediol dehydrogenase activity for the D/L/meso stereoisomer is given in percent.

^b Threonine dehydrogenase activity.

^c This ADH from *C. beijerinckii* NRRL B593 has no homolog in *C. beijerinckii* NCIMB 8052, from which Cb-ACR was derived.

^d ND, not determined.

Metal content. The metal content of purified Cb-ACR was determined by inductively coupled plasma atomic emission spectroscopy (ICP-AES) using buffer A as a blank. The analyses included the metal ions Ca²⁺, Cd²⁺, Cu²⁺, Mg²⁺, Mn²⁺, Ni²⁺, and Zn²⁺. The effect of metal ions on acetoin reductase activity was determined using different metal salts (CaCl₂, CoCl₂, FeCl₃, FeSO₄, NiCl₂, MgCl₂, MnCl₂, and ZnCl₂) at a final concentration of 1 mM. To remove any divalent metals, the enzyme preparation was first preincubated in 1 mM EDTA at 37°C for 60 min, after which the EDTA was removed by a desalting column. Subsequently, the residual activity of the acetoin reductase was measured as described above. The activity of Cb-ACR without pretreatment with EDTA or addition of metal ions was defined as 100%.

Sequence and structure analysis. The secondary structure of Cb-ACR was predicted using Pspred (21). Phylogenetic analysis was performed by aligning the amino acid sequence of Cb-ACR with the amino acid sequences of known characterized reductases (Table 1) using T-Coffee (22). A bootstrapped phylogenetic tree was constructed using Clustal W (23) and displayed using the neighbor-joining method with NJPlot 1.0 (24).

Structural modeling. A structural model of Cb-ACR was built using the automatic protein structure prediction server of Phyre V2.0 with the modeling mode set to intensive (25). Intensive performs complete modeling of the entire protein using multiple templates and *ab initio* techniques. *Ab initio* techniques for structure prediction are generally unreliable, but they can provide valuable clues to structural features. Model reliability and accuracy were analyzed by QMEAN (26, 27). The QMEAN score ranges between 0 and 1 with higher values for better models. The QMEAN Z-score provides an estimate of the absolute quality of a model by relating it to reference structures solved by X-ray crystallography. Predicted models of low quality are expected to have strongly negative QMEAN Z-scores. The quality of the model was further analyzed using Ramachandran plot analysis (Procheck) (28) and WhatCheck (a subset of the WhatIf program) (29) (<http://swift.cmbi.ru.nl/servers/html/index.html>).

RESULTS AND DISCUSSION

Identification and cloning of potential acetoin reductase-encoding genes. The well-studied solvent-producing *C. acetobutylicum* is also known to produce acetoin but not 2,3-butanediol (9). In an effort to have *C. acetobutylicum* produce 2,3-butanediol, a metabolic engineering approach was done previously, requiring

the introduction of a heterologous acetoin reductase gene (10). The search for the desired ACR and the further characterization are described here. BLAST-P searches on the genome of another solventogenic clostridium, *C. beijerinckii* NCIMB 8052, using available ACR/BDH amino acid sequences, yielded a set of putative ACR/BDH genes. The highest scores were obtained with the acetylacetoin reductase/2,3-butanediol dehydrogenase gene from *Bacillus cereus* YUF-4 (17), which resulted in eight putative acetoin reductase-encoding genes, with identities ranging between 24% and 54%. These eight predicted acetoin reductases encoded by *CBEI_0223*, *CBEI_0528*, *CBEI_0544*, *CBEI_0685*, *CBEI_1464*, *CBEI_2243*, *CBEI_3864*, and *CBEI_3890* are all annotated in NCBI (<http://www.ncbi.nlm.nih.gov/>) as alcohol dehydrogenase. *CBEI_1464* showed the highest similarity (53%) to the *B. cereus* query and thus was the most likely candidate to possess acetoin reductase activity.

Six of the candidate acetoin reductase genes were successfully expressed in *E. coli*; the gene constructs of *CBEI_0528* and *CBEI_0544* failed to produce transformants in *E. coli* and were therefore no longer considered here. The initial screening in crude cell extracts showed that only *CBEI_1464* (Cb-ACR) exhibited significant acetoin reductase activity with racemic acetoin as the substrate (Fig. 1). Minor acetoin reductase activity was also found with *CBEI_0685*, *CBEI_2243*, and *CBEI_3864*, although these activities hardly exceeded the background.

In silico analysis of *C. beijerinckii* CBEI_1464. *C. beijerinckii* *CBEI_1464* encodes a protein of 360 amino acids and has a calculated molecular mass of approximately 38.8 kDa with a theoretical pI of 6.42 (<http://img.jgi.doe.gov/cgi-bin/w/main.cgi>). The protein belongs to COG1063 (cluster of orthologous groups of proteins), which comprises L-threonine dehydrogenase and related Zn-dependent dehydrogenases (<http://www.ncbi.nlm.nih.gov/COG/>). A BLAST-P analysis (<http://blast.ncbi.nlm.nih.gov/Blast.cgi>) discloses many putative GroES-containing, Zn-binding alcohol dehydrogenases from the genera *Clostridium* and *Bacillus*. The best hits with characterized enzymes concern those from the Gram-positive species *B. cereus* YUF-4 (56% identity), *Paenibacillus polymyxa* (50% iden-

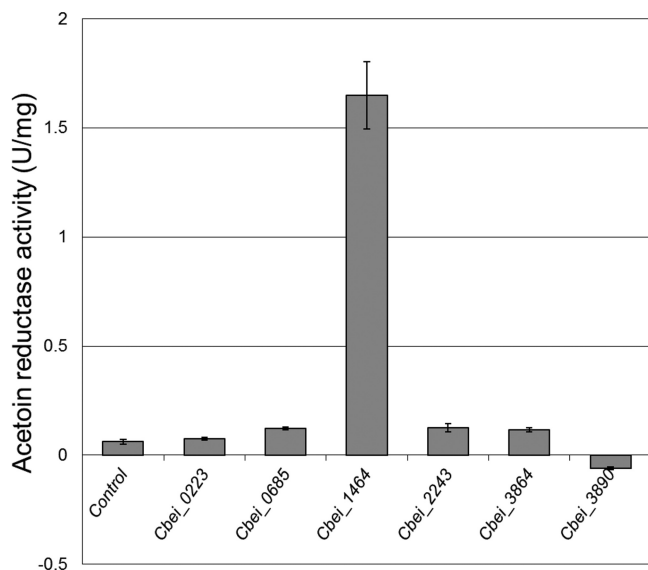


FIG 1 Acetoin reductase activity of six potential acetoin reductases from *C. beijerinckii* NCIMB 8052. The genes were heterologously expressed in *E. coli* BL21(DE3). Acetoin reductase activity was measured in crude cell extracts.

tity), *B. subtilis* subsp. *subtilis* (53% identity), and *Mycobacterium* strain B-009 (41% identity). Identification of the protein family and protein domains was performed using an Interpro scan from EMBL-EBI (<http://www.ebi.ac.uk/interpro/>). This scan confirmed that the protein is a member of the zinc-containing alcohol dehydrogenase superfamily (IPR002085), containing an N-terminal GroES-like alcohol dehydrogenase domain (IPR011032 and IPR013154) (amino acids [aa] 1 to 183), a conserved GroES-related zinc-binding domain (IPR02328) (aa 69 to 83), and an NAD(P)-binding alcohol dehydrogenase domain (IPR016040) (aa 175 to 295).

Purification of recombinant Cb-ACR. Cb-ACR was successfully purified to homogeneity from cell extract of *E. coli* BL21(DE3) containing pWUR450 by using three subsequent chromatographic columns, namely, a Matrex Gel Red A affinity column, a Ni-chelating affinity column, and a HiPrep desalting

column. SDS-PAGE analysis indicated an estimated molecular subunit mass of approximately 40 kDa (not shown). Size exclusion chromatography on a calibrated S200 column suggested that the quaternary structure of Cb-ACR is predominantly a homodimer, although a larger protein fraction, presumably representing tetramers, was also observed.

Optimal temperature and pH. The effect of temperature on Cb-ACR activity was studied for both the reduction and the oxidation reaction. The activity increased from 20°C to 80°C (Fig. 2A), with a temperature optimum for the reduction and oxidation reaction of around 68°C. This is remarkable, since the original host, *C. beijerinckii* NCIMB 8052, is a mesophilic microorganism. However, it has been observed more often that ADHs from *C. beijerinckii* are relatively stable at moderate temperatures (30–32). Also, closely related thermophilic *Clostridium* species are known to possess proteins with activity optima at higher temperatures (33). An Arrhenius analysis resulted in a linear plot in the temperature range of 20°C to 60°C (Fig. 2B), with a calculated activation energy for the formation of the enzyme/substrate complex of 96 kJ/mol. The linearity of the plot indicates that the conformation of Cb-ACR does not change throughout this temperature range.

To determine the optimal pH for both the reduction of acetoin and the oxidation of 2,3-butanediol, the activity of Cb-ACR was measured in a pH range of 5.5 to 10.0 (Fig. 2C). Cb-ACR displayed >70% of its maximal activity in the pH range of 6 to 7, with an optimal pH at approximately 6.5 for the reduction of acetoin. For the oxidation of 2,3-butanediol, >90% of its maximal activity was in the pH range of 9 to 9.5, with an optimal pH at approximately 9.5.

Substrate specificity and kinetics. Purified Cb-ACR was tested for multiple potential substrates. The specific reductase activity of Cb-ACR was found to be highest on D/L-acetoin (Table 2). Also, the conversions of diacetyl, 3-acetoxy-2-butanone, and acetol were shown to proceed with a relatively high activity (92%, 66%, and 46%, respectively). 2-Butanone showed a very low activity (2%). In the oxidative direction, the highest activities were found with diols with 2 adjacent hydroxyl groups, with D-2,3-butanediol and meso-2,3-butanediol performing best. The L-isomer of 2,3-butanediol did not show any activity. Some activity was also observed for 1,2-propanediol (24%), but compounds with

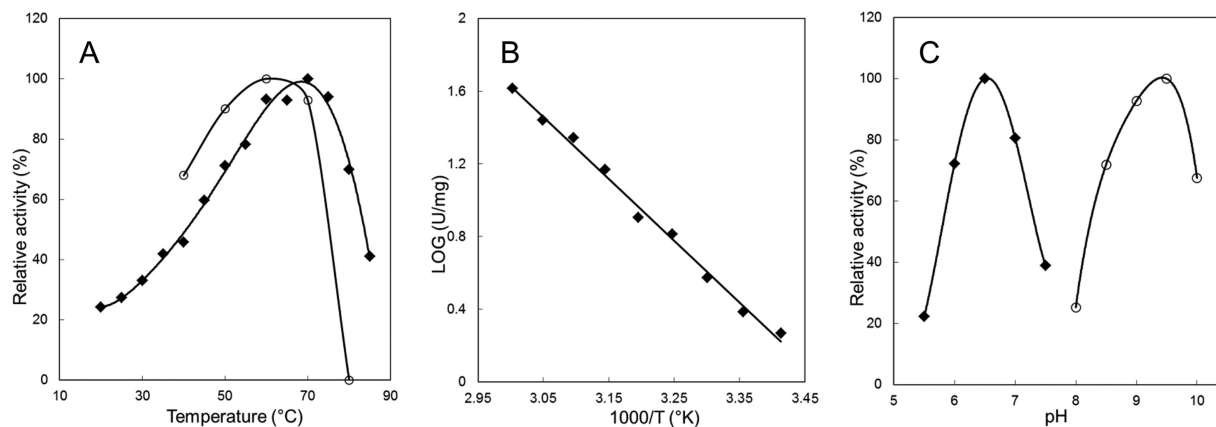
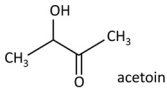
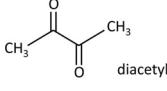
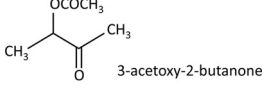
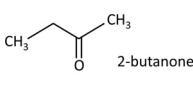
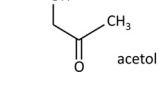


FIG 2 Effect of temperature and pH on acetoin reductase activity. (A) Effect of temperature; 20°C to 85°C for the reduction reaction (◆) and 40°C to 80°C for the oxidation reaction (○). (B) Arrhenius plot of the temperature dependence of the reduction reaction from 20°C to 60°C. (C) Effect of pH; pH 5.5 to 7.5 for the reduction reaction (◆) and 8.0 to 10.0 for the oxidation reaction (○).

TABLE 2 Substrate specificity of Cb-ACR^a

Substrate	Relative activity		
	%	±SE	
Reductive reaction			
Acetoin*	100	4	
Diacetyl	92	6	
3-Acetoxy-2-butanone*	66	4	
2-Butanone	2	3	
Acetol	46	1	
Oxidative reaction			
D(-)(2R,3R)-2,3-Butanediol	100	11	
L(+)(2S,3S)-2,3-Butanediol	0		
2,3-Butanediol*	80	4	
Meso-2,3-butanediol	99	7	
2-Butanol*	0		
1,2-Propanediol*	24	4	
1,3-Propanediol	0		
3-Amino-1,2-propanediol*	0		
1-Propanol	0		
2-Propanol	0		
Glycerol	1		
Ethanol	0		
Ethylene glycol	1		
L-Threonine	0		
D-Threonine	0		
L-Serine	0		
D-Sorbitol	0		
D-Xylitol	0		

^a The specific activity of Cb-ACR in the reductive and oxidative direction is shown. Activities are expressed as percentages of the most active substrate. Standard errors based on 3 or more replicates are shown. Structural formulas of the most active substrates in the reductive direction are shown. An asterisk indicates a racemic mixture.

more distant hydroxyl groups (1,3-propanediol and ethylene glycol) or a single hydroxyl group (2-butanol, 1-propanol, 2-propanol, and ethanol) showed no activity. Also, D- or L-threonine could not be used as a substrate. Altogether, these results indicate that enzyme activity requires a hydroxyl, keto, or acetoxy group, adjacent to the redox-active keto/hydroxyl group (Table 2 shows the structural formulas). The electronegative nature of the indicated groups suggests that they are probably involved in hydrogen bonding.

The specific activity of the D-2,3-butanediol dehydrogenation was 5.4-fold lower than the acetoin reduction (1.7 U/mg and 9.1 U/mg, respectively). With respect to the cofactor usage, Cb-ACR showed the highest activities with NADPH as the electron donor. A reasonable activity was, nevertheless, also obtained on NADH. The specific activity of the reaction with NADPH is about 2-fold higher and the apparent K_m value for NADPH was ~10-fold lower than those found for NADH (0.032 mM and 0.304 mM, respectively). This evidently results in ~20-fold-higher catalytic efficiency for the NADPH-dependent reaction (Table 3). Using racemic acetoin and NADPH, specific activities amounted to ~11 U/mg. The K_m for acetoin (0.4 to 0.5 mM) is not significantly different when NADH or NADPH is used as the electron donor.

Effect of metal ions and oxygen. Based on the *in silico* analysis, Cb-ACR is expected to be a member of the zinc-containing alcohol dehydrogenase superfamily. Inductively coupled plasma atomic emission spectroscopy (ICP-AES) confirmed the presence

TABLE 3 Kinetic data of purified Cb-ACR

Reaction	V_{max} (U · mg ⁻¹)	K_m (mM)		k_{cat}/K_m (s ⁻¹ · mM ⁻¹)
		Acetoin	NAD(P)H	
Acetoin + NADPH	10.6 ± 0.6	0.39 ± 0.11	0.032 ± 0.003	214 ± 23
Acetoin + NADH	5.41 ± 0.1	0.48 ± 0.05	0.304 ± 0.024	11.5 ± 0.94

of approximately two zinc atoms and one calcium per monomer of Cb-ACR. Remarkably, the residual activity in the control after preincubation in the presence of EDTA remained 100%. This suggests that the zinc molecules are tightly bound to the Cb-ACR or that they do not have a catalytic role. Addition of most salts and metals caused no significant inhibition or activation of Cb-ACR. Further research is needed to explain the presence of the calcium atom. Addition of extra calcium did not result in differences in specific activities.

Furthermore, Cb-ACR was found to be oxygen sensitive, with a half-life of approximately 6 h (aerobic at 0°C). However, addition of common reducing agents like dithiothreitol (DTT) or β-mercaptoethanol caused a strong inhibition. Possibly, these compounds (respectively, C₄ and C₂) mimic the substrate acetoin and as such occupy the active site, resulting in inhibition. Moreover, both mercaptoethanol and DTT contain an electronegative group (S) adjacent to the carbon containing the hydroxyl group (see below), as was also seen for the diols, discussed above. Inhibition by β-mercaptoethanol has been described also for the meso-BDH of *K. pneumoniae*, where the crystal structure revealed that mercaptoethanol specifically binds to the active site, forming hydrogen bonds to Gln₁₄₀ and Gly₁₈₃ (34). Also, for DTT and other thiols, strong inhibition has been reported for a sheep liver sorbitol dehydrogenase, where DTT forms a tight ternary complex with the enzyme-NAD complex (35). When tris(2-carboxyethyl)phosphine (TCEP) was used as a reducing agent, inhibition did not occur (19). In the presence of TCEP, the oxygen sensitivity was severely diminished, especially when stored at -20°C.

The oxygen-sensitive nature of the Cb-ACR might be caused by one or more of the 8 cysteines present in the primary sequence. However, all known ACRs contain several cysteine residues (ranging from 3 to 11), while a sensitivity to oxygen has never been reported, except for the ACR/BDH from the archaeon *Thermococcus guaymasensis* (36). Moreover, as discussed above, several of the cysteine residues are proposed to be involved in binding of the zinc ions. These residues are therefore conserved in ACRs, including those which are not oxygen sensitive. Cys₁₂₃ and Cys₁₉₁ are, however, unique to Cb-ACR (Fig. 3) and may therefore be responsible for the observed oxygen sensitivity. Also, the ACR/BDH from *T. guaymasensis* contains a cysteine in an unusual position, possibly explaining its oxygen sensitivity (36).

Cb-ACR in comparison to other characterized ACRs/BDHs. Although the currently available genome sequences harbor hundreds of closely related representatives of the zinc-containing alcohol dehydrogenase superfamily, only a limited number of ACRs/BDHs has been characterized in more detail. All closely related ACRs/BDHs are highly specific for the D-isomer (2R,3R) of 2,3-butanediol (Table 1). The more distantly related and smaller ACRs/BDHs from *K. pneumoniae* and homologs (not discussed in detail here) have been shown to be specific for meso-2,3-butanediol or the L-isomer (2S,3S) (13). As discussed recently by Yu et al., these clear differences in specificity can be associated with differ-

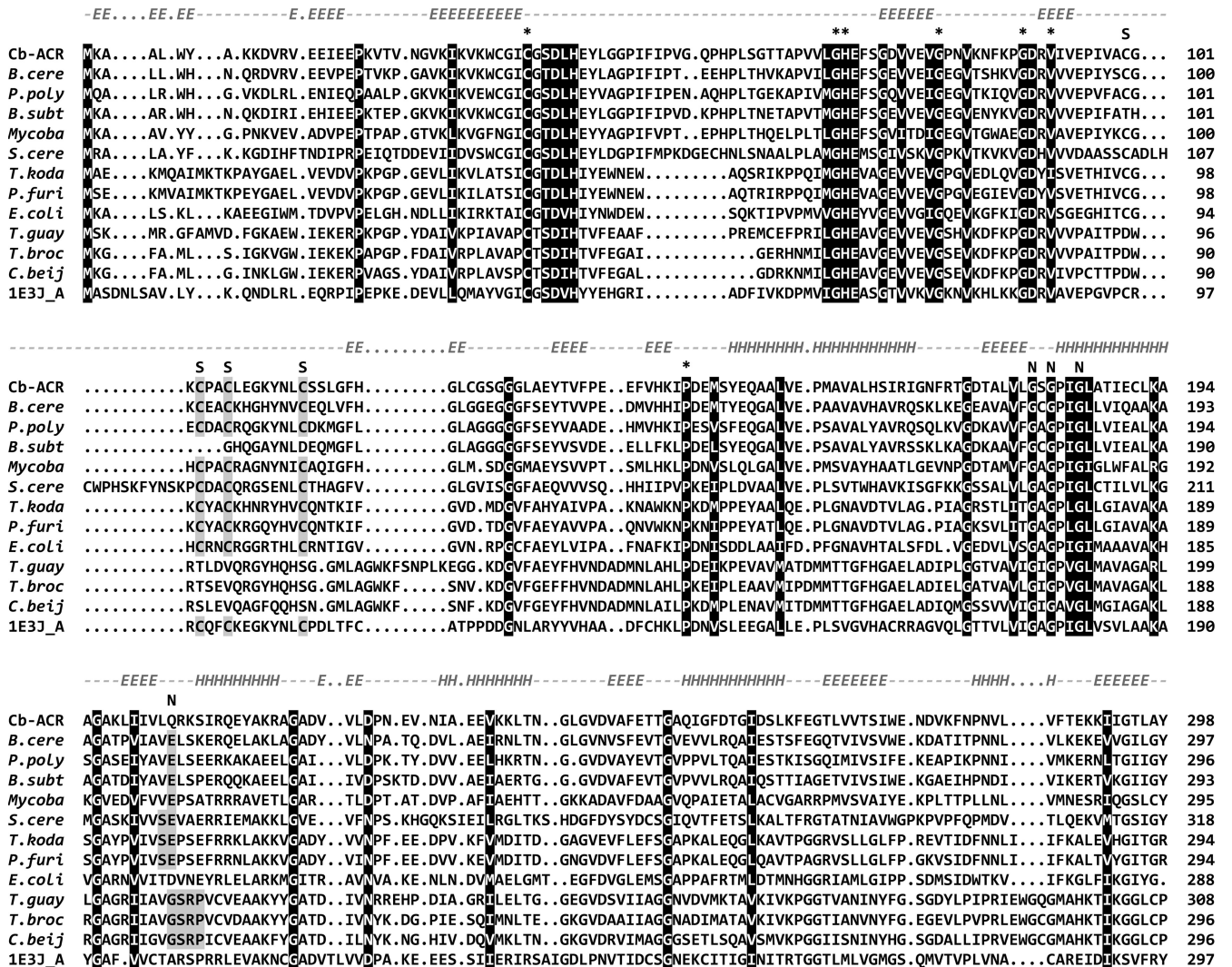


FIG 3 Multiple sequence alignment of Cb-ACR and other characterized close homologs. Gene identifiers of the genes can be found in Table 1. The sequence of the ketose reductase of *Bemisia argentifolii* (GI:4106363) was included because a three-dimensional structure was available (PDB 1E3J), which was used for the modeling of Cb-ACR. The sequences were aligned using the web-based T-Coffee program (22). Conserved residues involved in metal and NAD(P) binding are shaded in black. Asterisks indicate residues involved in binding of the catalytic and structural zinc. The secondary structure prediction of Cb-ACR (using the psipred program [59]) is shown above the alignment.

ent superfamilies, viz., the medium-chain dehydrogenase/reductase and the short-chain dehydrogenase/reductase superfamily (37). All of the medium-chain dehydrogenase/reductase representatives discussed here belong to COG1063 (Table 1), covering “threonine dehydrogenase and related Zn-dependent dehydrogenases.” According to the classification of Riveros-Rosas et al., COG1063 represents one of the families (polyol dehydrogenase) within macrofamily I and one which can be subdivided into 12 subfamilies, involved in various metabolic roles (38).

The alignment (Fig. 3) encompasses the closest orthologs, including a set of archaeal threonine dehydrogenases which belong to the same COG (1063). Conserved residues (shown with asterisks in the alignment) are those involved in binding of a catalytic zinc atom (Cys₃₇, His₇₀, and Glu₇₁) and those involved in NAD(P)⁺ binding (G₁₈₀XG₁₈₂XXG₁₈₅), as suggested by the identified Interpro domains. In addition to the residues that bind the catalytic zinc, a set of 4 conserved cysteines (Cys₁₀₀, Cys₁₀₃, Cys₁₀₆,

and Cys₁₁₄) is present in most sequences, which has been suggested to constitute the binding site of a structural zinc atom (12). This structural zinc binding site is, however, not present in the ACR/BDH (*ydjL*) of *B. subtilis* subsp. *subtilis* 168, which is closely related to the Cb-ACR. This observation is remarkable, as its primary sequence nicely aligns, except for the four missing cysteines. As yet, we have no explanation for this. Also, the BDHs of *T. brockii*, *T. guaymasensis*, and another *C. beijerinckii* strain (NRRL B593) do not contain these cysteine residues. The latter BDHs constitute a more distantly related group, as can be seen in the phylogenetic comparison (Fig. 4). In addition to the absence of the structural zinc, this group has also been shown to prefer NADP over NAD (Table 1). Structure analysis has indicated that the NADP specificity is determined by the residues Gly₁₉₈, Ser₁₉₉, Arg₂₀₀, and Tyr₂₁₈ (*T. brockii* numbering) (39–41). Indeed, most other sequences shown here contain other residues at these positions, e.g., the Gly is usually replaced by a Glu (Fig. 3). In this

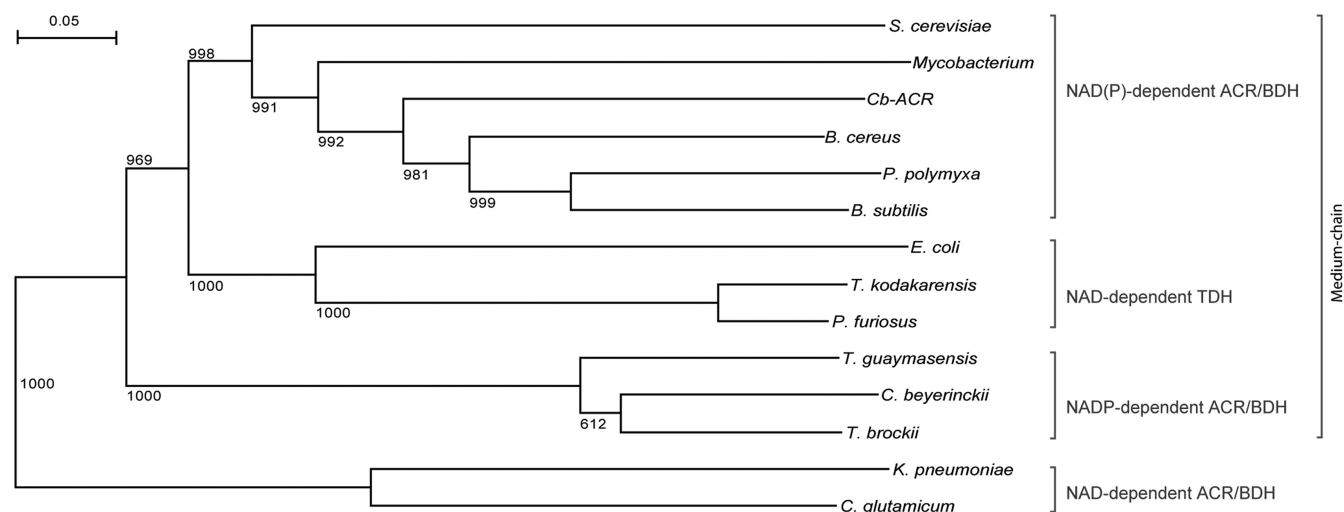


FIG 4 Phylogenetic tree of characterized ACRs/BDHs. Amino acid sequences used for the multiple alignment were also used to construct a phylogenetic tree, except that sequences of ACRs/BDHs that belong to a different superfamily, *viz.*, *K. pneumoniae* and *Corynebacterium glutamicum*, were added. The tree includes sequences of archaeal, bacterial, and eukaryotic origin, revealing the broad phylogenetic spreading of this group of enzymes. The different clades of NAD- and NADP-dependent enzymes and threonine dehydrogenases are indicated.

respect, it is remarkable that the Cb-ACR has a preference for NADP as well but does not contain the indicated residues. The gene sequence of Cb-ACR contains a Gln instead of the Gly or Glu.

Based on the alignment (Fig. 3), the phylogenetic tree (Fig. 4), and the data in Table 1, we show that the medium-chain ACRs/BDHs (COG1063) can be subdivided into three clades, which differ in cofactor specificity, quaternary structure, and catalytic activity. *T. guaymasensis*, *T. brockii*, and *C. beijerinckii* (CbADH) require NADP(H) and have an α_4 tetrameric structure. The archaeal enzymes from *Pyrococcus furiosus* and *Thermococcus kodakarensis* and the one from *E. coli* also have an α_4 structure but use NAD(H) and are able to convert threonine. These might be true threonine dehydrogenases, although the enzyme from *P. furiosus* also shows high activity on 2,3-butanediol (42). A third clade contains the Cb-ACR and related enzymes. All have a dimeric α_2 structure, and all are specific for NAD(H), except for the Cb-ACR, which can use NADP(H) as well (Table 1). Cb-ACR shows no activity on threonine. For the other members of this clade, threonine has not been tested. Thus, whether the absence of threonine dehydrogenase activity also holds for the other clade members remains to be investigated.

Structural modeling. Until now, no structure has been determined for any acetoin reductase of this superfamily. Hence, a structural model of Cb-ACR was built using the automatic protein structure prediction server of Phyre V2.0. Multiple fits with structural similarities were found, and based on heuristics to maximize confidence, percent identity, and alignment coverage, six templates (PDB 1e3j, 1p16, 1k0l, 4a10, 2dph, and 4a2c) were selected and used to model Cb-ACR. In addition, 4 residues were modeled *ab initio*. In the final model, 99% of residues were modeled at >90% confidence. Model reliability and accuracy were checked by QMEAN, resulting in the following scores: QMEAN score, 0.691; Z-score, -0.59. The QMEAN analysis included an image of the structure showing the regions with high error values. The majority of the model had low-error values, but three loops showed higher error values: Gly₄₇-Pro₆₅, Arg₂₀₅-Gln₂₁₀, and Pro₂₂₄-Ala₂₃₀. The Ramachandran plot (not shown) indicated that 96.3% of the

residues are in the most favored regions and additionally allowed regions. WhatCheck analysis showed that bond lengths and angles were found to deviate normally from the standard bond lengths and angles. Torsion angle evaluation showed only a few unusual residues. The backbone torsion angle evaluation, however, showed unusual conformations in loop Gly₄₇-Pro₆₅. Apparently, this loop is difficult to model and decreases the quality of the model. Although there are some concerns about the details of the structural model, we consider the obtained model useful to gain insight into the three-dimensional structure of Cb-ACR.

The Cb-ACR model structure has an overall fold very similar to that of other ADHs, despite sharing less than 35% protein sequence identity with those ADHs for which structures are known. As already concluded from the *in silico* analysis, the Cb-ACR structural model (Fig. 5) is comprised of two domains, a cofactor binding domain (residues 160 to 297) and a catalytic domain (residues 1 to 159 and 298 to 360), which are separated by a deep cleft. The cofactor binding domain has the characteristic α/β NAD(P) binding Rossmann fold composed of 6 β -strands and 6 accompanying α -helices (Fig. 5A) (43). The catalytic domain also has an α/β -fold similar to that observed in other ADHs. By analogy to the *Bemisia argentifolii* ketose reductase (Ba-KR) (PDB 1e3j) (44), which was one of the templates used for the modeling, we can propose that Cb-ACR contains a catalytic zinc atom in the putative active site, which is located in the catalytic domain at the bottom of the cleft, and a structural zinc atom coordinated by four cysteine residues (Cys₁₀₀, Cys₁₀₃, Cys₁₀₆, and Cys₁₁₄). Furthermore, as in the Ba-KR, the Cb-ACR catalytic zinc is bound by the side chains of Cys₃₇, His₇₀, Glu₇₁, and a water molecule, in a variation of the zinc site generally found in ADHs. In addition, the proposed adenyl phosphate moiety (of NADP) binding site in Ba-KR is also conserved in the Cb-ACR structure (Fig. 5B) and consists of Arg₂₀₅ and Arg₂₀₉, which is in agreement with the observed preference of Cb-ACR for NADP. Also, the residues of the conserved NAD(P) binding motif GxGxxG (Fig. 3), composed of Gly₁₈₀, Gly₁₈₂, and Gly₁₈₅, are accessible in the model and enable binding of the nucleotide.

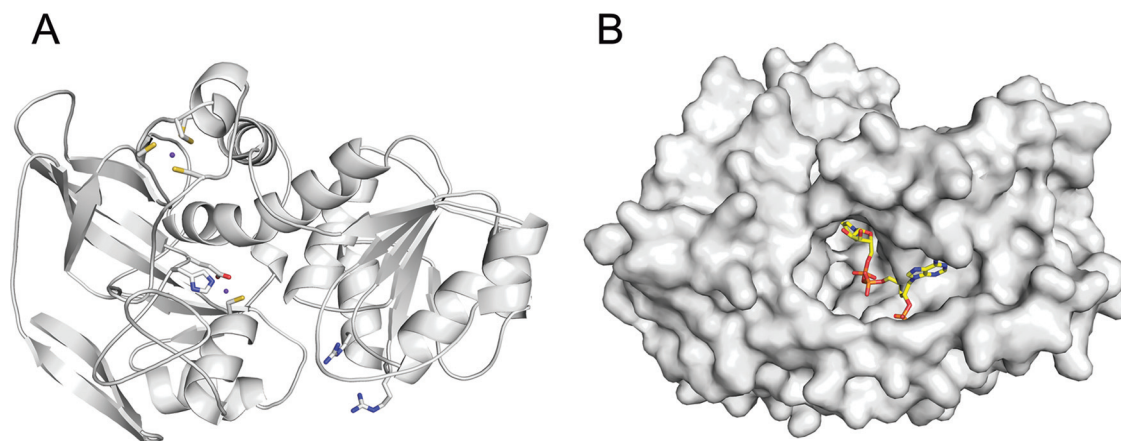


FIG 5 Three-dimensional model of Cb-ACR. (A) Overall structure of Cb-ACR. Residues Cys₃₇, His₇₀, and Glu₇₁ of the catalytic site are indicated. The catalytic and structural zinc molecules (purple spheres) were modeled into the structure using a superposition with *B. argentifolii* Ba-KR ADH (PDB 1e3j) (44). The four cysteines (Cys₁₀₀, Cys₁₀₃, Cys₁₀₆, and Cys₁₁₄) binding the structural zinc and the conserved arginines (Arg₂₀₅ and Arg₂₀₉) involved in binding the adenyl phosphate moiety of NADP are indicated. (B) Surface representation of Cb-ACR model. An NADP molecule was modeled into the structure using a superposition with *T. brockii* TBADH (PDB 1ykf) (41), giving an indication of how NADP is bound. These images were generated using PyMOL (PyMOL Molecular Graphics System, Version 1.2r3pre; Schrödinger, LLC).

Cofactor specificity. With respect to the cofactor usage, Cb-ACR showed the highest activities with NADPH as electron donor. The preference for NADP(H) is rather unexpected. All close homologs prefer NAD(H) over NADP(H) (Table 1), and NADP(H) dependence has been shown only for the more distantly related ACRs/BDHs from *T. guaymasensis*, *T. brockii*, and *C. beijerinckii* (Table 1; Fig. 4). In *B. cereus* YUF-4, two acetylacetoins reductases (AACRI and AACRII) have been described, with AACRI showing a preference for NADP(H) and AACRII showing a preference for NAD(H) (45). However, for AACRI no amino acid sequence is known, making it impossible to assess its relatedness to Cb-ACR. But according to the properties described by Hosaka et al. (45), AACRI is likely to belong to a different ACR/BDH family. NAD(H)-dependent AACRII, evidently, resembles the Cb-ACR, as it was used as a query to screen the *C. beijerinckii* genome. The unusual preference of Cb-ACR for NADP(H) might be a reflection of a different physiological role, e.g., the NADPH dependence suggests that Cb-ACR might fulfill an anabolic rather than a catabolic role.

The structural basis for the preference of NADP over NAD has been discussed by Baker et al. (46). The primary determinant is the residue at position 204 (CBEI_1464 numbering). A small and neutral residue at this position (G, A, or S) leaves room for the phosphate group of NADP, whereas dehydrogenases specific for NAD have a larger negatively charged residue (E or D) at this position. Indeed, the alignment shown in Fig. 3 appears to confirm this theory. All NAD(H)-dependent ACRs/BDHs have an E or a D at the indicated position, while the NAD(P)-dependent enzymes have a G. Cb-ACR is somewhat unusual in this respect, as it has a bulky glutamine (Q) at position 204. Apparently, the absence of a negative charge is sufficient to accommodate NADP(H). It has been suggested that the nearby presence of one or two basic residues is also important for NADP(H) specificity (47). This is indeed the case for the Cb-ACR, where the Gln₂₀₄ is followed by two arginines, Arg₂₀₅ and Arg₂₀₉. Also, the NADP(H)-dependent Ba-KR from *B. argentifolii*, whose structure was used to construct the Cb-ACR structural model, contains a neutral ala-

nine at the determining position and also two arginines (Arg₂₀₀ and Arg₂₀₄) in the vicinity.

Possible physiological and industrial role of Cb-ACR. As to the physiological role of Cb-ACR, it is interesting that CBEI_1464 clusters with a putative oxidoreductase (CBEI_1466) and a sigma54-specific transcriptional regulator from the Fis family (CBEI_1463). Several gene pairs that are homologous to the genes encoding CBEI_1463 and Cb-ACR are conserved within several species of the Firmicutes phylum. A BLAST-P search indicated that CBEI_1463 is similar to the *aco* operon expression regulatory protein (AcoR) of *Alcaligenes eutrophus* H16 and *Bacillus subtilis* (48, 49). The *aco* operon is known to code for subunits of an acetoin dehydrogenase, involved in the catabolism of acetoin as a carbon source. *B. subtilis* secretes acetoin in the medium, but after depletion of an external C source, it is able to use acetoin as a carbon source again by expressing its *aco* operon (48). The expression of this *aco* operon is regulated by *acoR*, which is highly similar to CBEI_1463. In *Clostridium magnum*, an acetoin dehydrogenase enzyme system, resembling the one encoded by the *aco* operon of *B. subtilis*, is described, which has also a similar AcoR-like protein (50). The presence of CBEI_1463 suggests that Cb-ACR of *C. beijerinckii* might be involved in the degradation of 2,3-butanediol to acetoin, which is then catabolized as in *C. magnum* and *B. subtilis*. However, an acetoin dehydrogenase complex as found in *C. magnum* and *B. subtilis* is not present in *C. beijerinckii*. A recent genome-wide transcriptional analysis of *C. beijerinckii* by whole-transcriptome shotgun sequencing (RNA-Seq) technology revealed that CBEI_1464 is significantly expressed, especially during the solventogenic phase (51). This suggests that Cb-ACR might have a role in the formation of an alcohol. Alternatively, as discussed above, the NADP-dependence points to a more anabolic role of Cb-ACR. *C. beijerinckii* is, however, not able to produce acetoin, which agrees with the fact that a gene for an acetolactate decarboxylase is missing. Altogether, this leaves the role of Cb-ACR in *C. beijerinckii* enigmatic.

Unlike *C. beijerinckii*, *C. acetobutylicum* does have the capacity to produce acetoin, but not 2,3-butanediol (2). By expression of

CBEL_1464 in *C. acetobutylicum*, it has recently been shown that Cb-ACR indeed accomplishes *in vivo* the stoichiometric conversion of acetoin to 2,3-butanediol (10). Future research continues on the use of the engineered *C. acetobutylicum* (Cb-ACR) strain. Its capacity to produce 2,3-butanediol is a first step toward a 2-butanol-producing strain. 2-Butanol is a potential biofuel, with an energy content similar to that of 1-butanol but with less toxicity to the producing strain (1).

ACKNOWLEDGMENTS

This project is financially supported by the Netherlands Ministry of Economic Affairs and the B-Basic partner organizations (www.b-basic.nl) through B-Basic, a public-private NWO-ACTS (Advanced Chemical Technologies for Sustainability) program.

REFERENCES

- Lopez Contreras AM, Kuit W, Siemerink MAJ, Kengen SWM, Springer J, Claassen PAM. 2010. Production of longer-chain alcohols from biomass—butanol, isopropanol and 2,3-butanediol, p 415–460. In Waldron K (ed), *Bioalcohol production*. Woodhead Publishing Ltd, Cambridge, United Kingdom.
- Jones DT, Woods DR. 1986. Acetone-butanol fermentation revisited. *Microbiol. Rev.* 50:484–524.
- Doremus MG, Linden JC, Moreira AR. 1985. Agitation and pressure effects on acetone-butanol fermentation. *Biotechnol. Bioeng.* 27:852–860. <http://dx.doi.org/10.1002/bit.260270615>.
- Ji XJ, Huang H, Ouyang PK. 2011. Microbial 2,3-butanediol production: a state-of-the-art review. *Biotechnol. Adv.* 29:351–364. <http://dx.doi.org/10.1016/j.biotechadv.2011.01.007>.
- Xiao Z, Xu P. 2007. Acetoin metabolism in bacteria. *Crit. Rev. Microbiol.* 33:127–140. <http://dx.doi.org/10.1080/10408410701364604>.
- Schink B. 1984. Fermentation of 2,3-butanediol by *Pelobacter carbinolicus* sp-nov and *Pelobacter propionicus* sp-nov, and evidence for propionate formation from C-2 compounds. *Arch. Microbiol.* 137:33–41. <http://dx.doi.org/10.1007/BF00425804>.
- Hohn-Bentz H, Radler F. 1978. Bacterial 2,3-butanediol dehydrogenases. *Arch. Microbiol.* 116:197–203. <http://dx.doi.org/10.1007/BF00406037>.
- Syu MJ. 2001. Biological production of 2,3-butanediol. *Appl. Microbiol. Biotechnol.* 55:10–18. <http://dx.doi.org/10.1007/s002530000486>.
- Wardwell SA, Yang YT, Chang HY, San KY, Rudolph FB, Bennett GN. 2001. Expression of the *Klebsiella pneumoniae* CG21 acetoin reductase gene in *Clostridium acetobutylicum* ATCC 824. *J. Ind. Microbiol. Biotechnol.* 27:220–227. <http://dx.doi.org/10.1038/sj.jim.7000179>.
- Siemerink MAJ, Kuit W, Lopez Contreras AM, Eggink G, van der Oost J, Kengen SWM. 2011. D-2,3-Butanediol production due to heterologous expression of an acetoin reductase in *Clostridium acetobutylicum*. *Appl. Environ. Microbiol.* 77:2582–2588. <http://dx.doi.org/10.1128/AEM.01616-10>.
- Radianingtyas H, Wright PC. 2003. Alcohol dehydrogenases from thermophilic and hyperthermophilic archaea and bacteria. *FEMS Microbiol. Rev.* 27:593–616. [http://dx.doi.org/10.1016/S0168-6445\(03\)00068-8](http://dx.doi.org/10.1016/S0168-6445(03)00068-8).
- Reid MF, Fewson CA. 1994. Molecular characterization of microbial alcohol dehydrogenases. *Crit. Rev. Microbiol.* 20:13–56. <http://dx.doi.org/10.3109/10408419409113545>.
- Ui S, Okajima Y, Mimura A, Kanai H, Kobayashi T, Kudo T. 1997. Sequence analysis of the gene for and characterization of D-acetoin forming meso-2,3-butanediol dehydrogenase of *Klebsiella pneumoniae* expressed in *Escherichia coli*. *J. Ferment. Bioeng.* 83:32–37. [http://dx.doi.org/10.1016/S0922-338X\(97\)87323-0](http://dx.doi.org/10.1016/S0922-338X(97)87323-0).
- Brouns SJ, Turnbull AP, Willems HL, Akerboom J, van der Oost J. 2007. Crystal structure and biochemical properties of the D-arabinose dehydrogenase from *Sulfolobus solfataricus*. *J. Mol. Biol.* 371:1249–1260. <http://dx.doi.org/10.1016/j.jmb.2007.05.097>.
- Shiloach J, Fass R. 2005. Growing *E. coli* to high cell density—a historical perspective on method development. *Biotechnol. Adv.* 23:345–357. <http://dx.doi.org/10.1016/j.biotechadv.2005.04.004>.
- Altschul SF, Madden TL, Schaffer AA, Zhang J, Zhang Z, Miller W, Lipman DJ. 1997. Gapped BLAST and PSI-BLAST: a new generation of protein database search programs. *Nucleic Acids Res.* 25:3389–3402. <http://dx.doi.org/10.1093/nar/25.17.3389>.
- Hosaka T, Ui S, Ohtsuki T, Mimura A, Ohkuma M, Kudo T. 2001. Characterization of the NADH-linked acetylacetoin reductase/2,3-butanediol dehydrogenase gene from *Bacillus cereus* YUF-4. *J. Biosci. Bioeng.* 91:539–544. [http://dx.doi.org/10.1016/S1389-1723\(01\)80170-5](http://dx.doi.org/10.1016/S1389-1723(01)80170-5).
- Brouns SJ, Smits N, Wu H, Snijders AP, Wright PC, de Vos WM, van der Oost J. 2006. Identification of a novel alpha-galactosidase from the hyperthermophilic archaeon *Sulfolobus solfataricus*. *J. Bacteriol.* 188:2392–2399. <http://dx.doi.org/10.1128/JB.188.7.2392-2399.2006>.
- Getz EB, Xiao M, Chakrabarty T, Cooke R, Selvin PR. 1999. A comparison between the sulfhydryl reductants tris(2-carboxyethyl)phosphine and dithiothreitol for use in protein biochemistry. *Anal. Biochem.* 273:73–80. <http://dx.doi.org/10.1006/abio.1999.4203>.
- Bradford MM. 1976. A rapid and sensitive method for the quantitation of microgram quantities of protein utilizing the principle of protein-dye binding. *Anal. Biochem.* 72:248–254. [http://dx.doi.org/10.1016/0003-2697\(76\)90527-3](http://dx.doi.org/10.1016/0003-2697(76)90527-3).
- McGuffin LJ, Bryson K, Jones DT. 2000. The PSIPRED protein structure prediction server. *Bioinformatics* 16:404–405. <http://dx.doi.org/10.1093/bioinformatics/16.4.404>.
- Notredame C, Higgins DG, Heringa J. 2000. T-Coffee: a novel method for fast and accurate multiple sequence alignment. *J. Mol. Biol.* 302:205–217. <http://dx.doi.org/10.1006/jmbi.2000.4042>.
- Larkin MA, Blackshields G, Brown NP, Chenna R, McGettigan PA, McWilliam H, Valentin F, Wallace IM, Wilm A, Lopez R, Thompson JD, Gibson TJ, Higgins DG. 2007. Clustal W and Clustal X version 2.0. *Bioinformatics* 23:2947–2948. <http://dx.doi.org/10.1093/bioinformatics/btm404>.
- Perriere G, Gouy M. 1996. WWW-query: an on-line retrieval system for biological sequence banks. *Biochimie* 78:364–369. [http://dx.doi.org/10.1016/0300-9084\(96\)84768-7](http://dx.doi.org/10.1016/0300-9084(96)84768-7).
- Kelley LA, Sternberg MJE. 2009. Protein structure prediction on the Web: a case study using the Phyre server. *Nat. Protoc.* 4:363–371. <http://dx.doi.org/10.1038/nprot.2009.2>.
- Benkert P, Kunzli M, Schwede T. 2009. QMEAN server for protein model quality estimation. *Nucleic Acids Res.* 37:W510–W514. <http://dx.doi.org/10.1093/nar/gkp322>.
- Benkert P, Tosatto SCE, Schomburg D. 2008. QMEAN: a comprehensive scoring function for model quality assessment. *Proteins Struct. Funct. Bioinformatics* 71:261–277. <http://dx.doi.org/10.1002/prot.21715>.
- Laskowski RA, MacArthur MW, Moss DS, Thornton JM. 1993. Procheck—a program to check the stereochemical quality of protein structures. *J. Appl. Crystallogr.* 26:283–291. <http://dx.doi.org/10.1107/S0021889892009944>.
- Hoof RWV, Vriend G, Sander C, Abola EE. 1996. Errors in protein structures. *Nature* 381:272. <http://dx.doi.org/10.1038/381272a0>.
- Bogin O, Peretz M, Hacham Y, Korkhin Y, Frolow F, Kalb AJ, Burstein Y. 1998. Enhanced thermal stability of *Clostridium beijerinckii* alcohol dehydrogenase after strategic substitution of amino acid residues with prolines from the homologous thermophilic *Thermoanaerobacter brockii* alcohol dehydrogenase. *Protein Sci.* 7:1156–1163. <http://dx.doi.org/10.1002/pro.5560070509>.
- Ismail AA, Zhu CX, Colby GD, Chen JS. 1993. Purification and characterization of a primary-secondary alcohol dehydrogenase from two strains of *Clostridium beijerinckii*. *J. Bacteriol.* 175:5097–5105.
- Li C, Heatwole J, Soelaiman S, Shoham M. 1999. Crystal structure of a thermophilic alcohol dehydrogenase substrate complex suggests determinants of substrate specificity and thermostability. *Proteins* 37:619–627. [http://dx.doi.org/10.1002/\(SICI\)1097-0134\(19991201\)37:4<619::AID-PROT12>3.0.CO;2-H](http://dx.doi.org/10.1002/(SICI)1097-0134(19991201)37:4<619::AID-PROT12>3.0.CO;2-H).
- Demain AL, Newcomb M, Wu JH. 2005. Cellulase, clostridia, and ethanol. *Microbiol. Mol. Biol. Rev.* 69:124–154. <http://dx.doi.org/10.1128/MMBR.69.1.124-154.2005>.
- Otagiri M, Kuru G, Ui S, Takusagawa Y, Ohkuma M, Kudo T, Kusunoki M. 2001. Crystal structure of meso-2,3-butanediol dehydrogenase in a complex with NAD⁺ and inhibitor mercaptoethanol at 1.7 Å resolution for understanding of chiral substrate recognition mechanisms. *J. Biochem.* 129:205–208. <http://dx.doi.org/10.1093/oxfordjournals.jbchem.a002845>.
- Lindstad RI, McKinley-McKee JS. 1996. Reversible inhibition of sheep liver sorbitol dehydrogenase by thiol compounds. *Eur. J. Biochem.* 241:142–148. <http://dx.doi.org/10.1111/j.1432-1033.1996.0142t.x>.
- Ying X, Ma K. 2011. Characterization of a zinc-containing alcohol dehydrogenase with stereoselectivity from the hyperthermophilic archaeon *Thermococcus guaymasensis*. *J. Bacteriol.* 193:3009–3019. <http://dx.doi.org/10.1128/JB.01433-10>.

37. Yu B, Sun J, Bommareddy RR, Song L, Zeng AP. 2011. Novel (2R,3R)-2,3-butanediol dehydrogenase from potential industrial strain *Paenibacillus polymyxa* ATCC 12321. *Appl. Environ. Microbiol.* 77:4230–4233. <http://dx.doi.org/10.1128/AEM.02998-10>.
38. Riveros-Rosas H, Julian-Sanchez A, Villalobos-Molina R, Pardo JP, Pina E. 2003. Diversity, taxonomy and evolution of medium-chain dehydrogenase/reductase superfamily. *Eur. J. Biochem.* 270:3309–3334. <http://dx.doi.org/10.1046/j.1432-1033.2003.03704.x>.
39. Bowyer A, Mikolajek H, Stuart JW, Wood SP, Jamil F, Rashid N, Akhtar M, Cooper JB. 2009. Structure and function of the L-threonine dehydrogenase (TKTDH) from the hyperthermophilic archaeon *Thermococcus kodakaraensis*. *J. Struct. Biol.* 168:294–304. <http://dx.doi.org/10.1016/j.jsb.2009.07.011>.
40. Gonzalez E, Fernandez MR, Larroy C, Pares X, Biosca JA. 2001. Characterization and functional role of *Saccharomyces cerevisiae* 2,3-butanediol dehydrogenase. *Chem. Biol. Interact.* 130–132:425–434. [http://dx.doi.org/10.1016/S0009-2797\(00\)00282-9](http://dx.doi.org/10.1016/S0009-2797(00)00282-9).
41. Korshin Y, Kalb AJ, Peretz M, Bogin O, Burstein Y, Frolow F. 1998. NADP-dependent bacterial alcohol dehydrogenases: crystal structure, cofactor-binding and cofactor specificity of the ADHs of *Clostridium beijerinckii* and *Thermoanaerobacter brockii*. *J. Mol. Biol.* 278:967–981. <http://dx.doi.org/10.1006/jmbi.1998.1750>.
42. Machielsen R, van der Oost J. 2006. Production and characterization of a thermostable L-threonine dehydrogenase from the hyperthermophilic archaeon *Pyrococcus furiosus*. *FEBS J.* 273:2722–2729. <http://dx.doi.org/10.1111/j.1742-4658.2006.05290.x>.
43. Rossmann MG, Moras D, Olsen KW. 1974. Chemical and biological evolution of nucleotide-binding protein. *Nature* 250:194–199. <http://dx.doi.org/10.1038/250194a0>.
44. Banfield MJ, Salvucci ME, Baker EN, Smith CA. 2001. Crystal structure of the NADP(H)-dependent ketose reductase from *Bemisia argentifolii* at 2.3 Å resolution. *J. Mol. Biol.* 306:239–250. <http://dx.doi.org/10.1006/jmbi.2000.4381>.
45. Hosaka T, Ui S, Mimura A. 1999. Separation and properties of two acetylacetoin reductases from *Bacillus cereus* YUF-4. *Biosci. Biotechnol. Biochem.* 63:199–201. <http://dx.doi.org/10.1271/bbb.63.199>.
46. Baker PJ, Britton KL, Rice DW, Rob A, Stillman TJ. 1992. Structural consequences of sequence patterns in the fingerprint region of the nucleotide binding fold. Implications for nucleotide specificity. *J. Mol. Biol.* 228:662–671.
47. Carugo O, Argos P. 1997. NADP-dependent enzymes. I. Conserved stereochemistry of cofactor binding. *Proteins* 28:10–28.
48. Ali NO, Bignon J, Rapoport G, Debarbouille M. 2001. Regulation of the acetoin catabolic pathway is controlled by sigma L in *Bacillus subtilis*. *J. Bacteriol.* 183:2497–2504. <http://dx.doi.org/10.1128/JB.183.8.2497-2504.2001>.
49. Kruger N, Steinbuechel A. 1992. Identification of acoR, a regulatory gene for the expression of genes essential for acetoin catabolism in *Alcaligenes eutrophus* H16. *J. Bacteriol.* 174:4391–4400.
50. Kruger N, Oppermann FB, Lorenz H, Steinbuechel A. 1994. Biochemical and molecular characterization of the *Clostridium magnum* acetoin dehydrogenase enzyme system. *J. Bacteriol.* 176:3614–3630.
51. Wang Y, Li X, Mao Y, Blaschek HP. 2012. Genome-wide dynamic transcriptional profiling in *Clostridium beijerinckii* NCIMB 8052 using single-nucleotide resolution RNA-Seq. *BMC Genomics* 13:102. <http://dx.doi.org/10.1186/1471-2164-13-102>.
52. Nicholson WL. 2008. The *Bacillus subtilis* ydJL (bdhA) gene encodes acetoin reductase/2,3-butanediol dehydrogenase. *Appl. Environ. Microbiol.* 74:6832–6838. <http://dx.doi.org/10.1128/AEM.00881-08>.
53. Yan Y, Lee CC, Liao JC. 2009. Enantioselective synthesis of pure (R,R)-2,3-butanediol in *Escherichia coli* with stereospecific secondary alcohol dehydrogenases. *Org. Biomol. Chem.* 7:3914–3917. <http://dx.doi.org/10.1039/b913501d>.
54. Takeda M, Muranushi T, Inagaki S, Nakao T, Motomatsu S, Suzuki I, Koizumi J. 2011. Identification and characterization of a mycobacterial (2R,3R)-2,3-butanediol dehydrogenase. *Biosci. Biotechnol. Biochem.* 75:2384–2389. <http://dx.doi.org/10.1271/bbb.110607>.
55. Gonzalez E, Fernandez MR, Larroy C, Sola L, Pericas MA, Pares X, Biosca JA. 2000. Characterization of a (2R,3R)-2,3-butanediol dehydrogenase as the *Saccharomyces cerevisiae* YAL060W gene product. Disruption and induction of the gene. *J. Biol. Chem.* 275:35876–35885. <http://dx.doi.org/10.1074/jbc.M003035200>.
56. Bashir Q, Rashid N, Jamil F, Imanaka T, Akhtar M. 2009. Highly thermostable L-threonine dehydrogenase from the hyperthermophilic archaeon *Thermococcus kodakaraensis*. *J. Biochem.* 146:95–102. <http://dx.doi.org/10.1093/jb/mvp051>.
57. Boylan SA, Dekker EE. 1978. L-threonine dehydrogenase of *Escherichia coli* K-12. *Biochem. Biophys. Res. Commun.* 85:190–197. [http://dx.doi.org/10.1016/S0006-291X\(78\)80028-X](http://dx.doi.org/10.1016/S0006-291X(78)80028-X).
58. Peretz M, Bogin O, Tel-Or S, Cohen A, Li G, Chen JS, Burstein Y. 1997. Molecular cloning, nucleotide sequencing, and expression of genes encoding alcohol dehydrogenases from the thermophile *Thermoanaerobacter brockii* and the mesophile *Clostridium beijerinckii*. *Anaerobe* 3:259–270. <http://dx.doi.org/10.1006/anae.1997.0083>.
59. Jones DT. 1999. Protein secondary structure prediction based on position-specific scoring matrices. *J. Mol. Biol.* 292:195–202. <http://dx.doi.org/10.1006/jmbi.1999.3091>.